
GauS: Differentiable Scheduling Optimization via Gaussian Reparameterization

Yaohui Cai¹ Vesal Bakhtazad¹ Cunxi Yu² Zhiru Zhang¹

Abstract

Efficient operator scheduling is a fundamental challenge in software compilation and hardware synthesis. While recent differentiable approaches have sought to replace traditional ones like exact solvers or heuristics with gradient-based search, they typically rely on categorical distributions that fail to capture the ordinal nature of time and suffer from a parameter space that scales poorly. In this paper, we propose a novel differentiable framework, GauS, that models operator scheduling as a stochastic relaxation using Gaussian distributions, which fully utilize modern parallel computing devices like GPUs. By representing schedules as continuous Gaussian variables, we successfully capture the ordinal nature of time and reduce the optimization space by orders of magnitude. Our method is highly flexible to represent various objectives and constraints, which provides the first differentiable formulation for the complex pipelined scheduling problem. We evaluate our method on a range of benchmarks, demonstrating that GauS achieves Pareto-optimal results.

1. Introduction

The efficient scheduling of operations onto a finite set of resources, an NP-hard problem known as operator scheduling, is a fundamental challenge across the entire computing stack. In software compilation, it is the critical phase that determines the execution order of instructions to maximize instruction-level parallelism and minimize pipeline stalls (Lam, 1988). In hardware synthesis, it is the cornerstone of high-level synthesis (HLS) (Cong & Zhang, 2006; Ku & De Micheli, 2002; Radivojevic & Brewer, 1996), where it dictates the cycle-by-cycle behavior of custom logic and the allocation of physical functional units. At its core, the problem involves mapping a set of operations to a discrete set of time steps while minimizing a given cost function and honoring a set of constraints.

¹Cornell University ²University of Maryland, College Park.
Correspondence to: Yaohui Cai <yc2632@cornell.edu>.

As we transition into an era of massive-scale deep learning models and heterogeneous architectures, the complexity of scheduling tasks has scaled dramatically from hundreds to tens of thousands of nodes. Modern workloads, such as those targeting the Groq Tensor Streaming Processor (TSP) (Abts et al., 2020), require orchestrating thousands of functional units simultaneously to exploit massive data parallelism. Similarly, emerging Processing-in-Memory (PIM) architectures (Guo et al., 2025; Seshadri et al., 2017), present unique scheduling challenges where bit-serial execution across large memory arrays requires precise temporal and spatial specification of thousands of operations.

Historically, efforts to solve the operator scheduling problem have fallen into two disparate camps, neither of which fully satisfies the needs of modern large-scale systems (Leiserson & Saxe, 1991). On one hand, Integer Linear Programming (ILP) (Fan et al., 2005) and Satisfiability Modulo Theory (SMT) (Fan et al., 2008) solvers provide optimal solutions but suffer from exponential runtime complexity, making them impractical for realistic workloads (Amarú et al., 2015; Soi et al., 2025). On the other hand, heuristic-based methods, such as list scheduling (Parker et al., 1986; Kondratyev et al., 2011) and force-directed scheduling (FDS) (Verhaegh et al., 1992; Paulin & Knight, 1987), offer the speed required for large-scale graphs but often yield suboptimal results, as they lack a global view of the optimization space and struggle to balance competing constraints like memory footprint and communication overhead.

A promising third path has recently emerged: differentiable combinatorial optimization, which has been widely used in many real-world combinatorial problems (Bengio et al., 2021; Zhang et al., 2025; Cai et al., 2025; Lin et al., 2019). By relaxing discrete scheduling decisions into a continuous space, these methods transform the NP-hard combinatorial search into a smooth, differentiable landscape. This shift provides a holistic view of the global optimization problem and allows the problem to be solved by gradient descent and utilizing the modern ML ecosystem including parallel computing devices like GPUs. While GS-Schedule (Liu et al., 2024) as an early attempt in this domain successfully proved the feasibility of differentiable optimization for scheduling using categorical relaxations (i.e., Gumbel-Softmax), it does not fully utilize the parallelism of GPUs and the number of parameters requiring optimization increases linearly with

respect to the depth (D) and size ($|V|$) of the graph.

In this paper, we introduce GauS, a differentiable Gaussian reparameterization Scheduling framework. We model the execution step of each operator as a continuous random variable following a Gaussian distribution $X \sim \mathcal{N}(\mu, \sigma^2)$, where the mean (μ) represents the expected schedule step and the standard deviation (σ) represents the uncertainty. Under this formulation, the number of parameters requiring optimization reduces to $2|V|$. The probability density function (PDF) of random variables provides a smooth and continuous proxy for discrete placement. Because of the properties of Gaussian distribution, we can represent a wide spectrum of expectations of objectives and constraint violations as differentiable functions of the Gaussian parameters (μ and σ). By minimizing the weighted sum of them, the original discrete combinatorial scheduling problem is essentially transformed to a continuous problem that can be efficiently solved by gradient descent. Our contributions are summarized as follows:

Novel Representation: This is the first work using Gaussian reparameterization in operator scheduling, which naturally encodes temporal proximity; as the mean μ shifts, the probability mass moves smoothly across adjacent steps, providing the optimizer with a much clearer signal for local refinement. The parameter space is also massively reduced compared to previous work.

Differentiable Flexibility: Utilizing the properties of the Gaussian distribution, we derive differentiable expressions for distinct complex objectives and constraints. Consequently, GauS can be naturally used to model pipelined scheduling (Lam, 1988; Rau & Glaeser, 1981).

Through extensive empirical evaluation on both synthetic and realistic benchmarks, we demonstrate that our method consistently produces the Pareto-optimal frontier of speed and quality. Compared to previous differentiable method and commercial solvers, GauS achieves equivalent solution quality while one to two orders of magnitude faster

2. Preliminaries

2.1. Scheduling Problem

Scheduling is the process of assigning a set of operations to specific time steps, while satisfying given constraints and optimizing for performance objectives. In this section, we formalize the objectives and constraints for both regular and pipelined scheduling.

2.1.1. REGULAR SCHEDULING

A workload is represented as a directed acyclic graph (DAG), $G = (V, E)$, where vertices $V = \{v_1, \dots, v_n\}$ represent computational operations and edges E denote data depen-

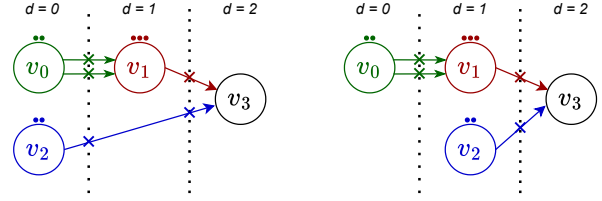


Figure 1. **Impact of optimization objectives on scheduling** — Impact of optimization objectives on scheduling. Nodes v_i (operators) show resource requirements r_i (number of dots) and bitwidths of storage units required b_i (number of arrows). Max depth (D) sets to 3. Left schedule minimizes resources ($\mathcal{L}_{res} = 4, \mathcal{L}_{mem} = 3$); right schedule minimizes memory footprint ($\mathcal{L}_{res} = 5, \mathcal{L}_{mem} = 2$).

dencies. In a regular scheduling problem, each operator v_i is assigned a discrete start time step $s_i \in \mathbb{N}$

Dependency constraint (Dep). The consumer v_j cannot begin until the producer completes its execution:

$$\underline{\text{Dep}}: \forall v_i, v_j \in E, \quad s_i + \text{Lat}(v_i) \leq s_j \quad (1)$$

where $\text{Lat}(v_i)$ is the execution latency of v_i . In contexts allowing *operation chaining*, where multiple operations with zero latency can be scheduled in the same step. Then this simplifies to $s_i \leq s_j$. For the sake of simplicity, we assume $\text{Lat}(v_i) = 1, \forall i$ in the remaining discussion.

Latency constraint (Lat) ensures the schedule length does not exceed a predefined limit D :

$$\underline{\text{Lat}}: \max s_i \leq D \quad (2)$$

Resource usage. Let r_i denote the resource demand of operator v_i . The resource usage at step d , $\text{Res}(d)$ is the sum of resources required for all operators active at step d , and the global resource usage is the maximum resource usage over all steps:

$$\text{Res}(d) = \sum_{v_i \in V} r_i \cdot \mathbb{I}[d_i = d] \quad (3a)$$

$$\mathcal{L}_{Res} = \max_d \text{Res}(d) \quad (3b)$$

Here $\mathbb{I}[C]$ is the indicator function, which outputs 1 when condition C is met and 0 otherwise.

Memory Footprint. To carry data across steps, operator v_i utilizes b_i storage units to store its output. Depending on the problem settings, storage units could be registers, SRAM, or DRAM. A storage unit is occupied from the step s_i until the step of its latest successor starts. Let $\text{succ}(v_i) = \{v_j \mid (v_i, v_j) \in E\}$ denote the set of immediate successors of v_i . The memory usage at step d is the sum of all active storage units which is required by all operators v_i scheduled at or before step d whose outputs are used by at least one operator

scheduled after step d . And the global memory footprint is the maximum memory usage over all step¹:

$$Mem(d) = \sum_{v_i \in V} b_i \cdot \mathbb{I} \left[s_i \leq d < \max_{v_j \in succ(v_i)} s_j \right] \quad (4a)$$

$$\mathcal{L}_{Mem} = \max_d Mem(d) \quad (4b)$$

Figure 1 demonstrates how different objectives impact the schedule of the same workload. A resource usage optimized schedule is on the left and a storage unit optimized schedule is on the right.

2.1.2. MODULO SCHEDULING

For high-throughput applications, *modulo scheduling* (Rau & Glaeser, 1981; Lam, 1988) achieves pipelined execution by starting a new loop iteration (or function invocation) every *initiation interval* (Π) steps. Because schedules from consecutive iterations overlap, the lifetimes of an operator and its output are wrapped within the initiation interval, which affects the resource requirements. Consequently, an operator scheduled at any step d such that $d = t + k \cdot \Pi$, $k \geq 0$, will demand resources ($MRes$) and occupy storage units ($MMem$) at time step t , $0 \leq t < \Pi$:

$$MRes(t) = \sum_k Res(t + k \cdot \Pi) \quad (5a)$$

$$MMem(t) = \sum_k Mem(t + k \cdot \Pi) \quad (5b)$$

Recurrence Constraint (Rec): With loop-carried dependencies between iterations, a back-edge from v_j to v_i with a distance k (iterations) represents the output from v_j is required for a v_i after k iterations. This constraint effectively sets a deadline for operator v_j relatively to the operator v_i .

$$\text{Rec: } s_i + k \cdot \Pi \geq s_j + \text{Lat}(v_j) \quad (6)$$

2.2. Scheduling Algorithms

Exact approaches typically formulate scheduling as an integer linear programming (ILP) (Hwang et al., 2002; Gebotys & Elmasry, 1993; Fan et al., 2005), boolean satisfiability (SAT) (Fan et al., 2008; Zhang et al., 2004). While these methods guarantee an optimal solution by exhaustively searching the solution space, they are fundamentally limited by the NP-hard nature of the problem. As the complexity of the problem grows, the number of constraints and variables grows exponentially. Consequently, exact solvers often fail to converge to a feasible solution within reasonable time-frames for large-scale, realistic graphs.

¹We add an explicit sink node as a successor for all leaf nodes (nodes without successors) to ensure their outputs are also carried toward the end.

Heuristics have been widely adopted to bridge the scalability gap of exact solvers. Basic baselines include as-soon-as-possible (ASAP) and as-late-as-possible (ALAP) scheduling, which provide the earliest and latest time slots for each operation. *List Scheduling* (Parker et al., 1986; Kondratyev et al., 2011) greedily assigns operations to steps based on a priority function, such as critical path depth. *Force-Directed Scheduling* (FDS) (Verhaegh et al., 1992; Paulin & Knight, 1987) offers a more sophisticated approach by modeling the scheduling process as a system of imaginary forces. By calculating *attraction* and *repulsion* based on resource demand distributions across the timeline, FDS attempts to balance utilization by shifting nodes toward steps with lower contention. However, despite their execution speed, these heuristics are inherently local and greedy. Because they make irreversible decisions step-by-step or node-by-node, they often struggle to optimize for global, non-linear objectives such as peak memory footprint or complex, cross-iteration pipelining constraints.

Furthermore, for *modulo scheduling*, its periodic nature introduces global cyclic coupling. When combined with recurrent constraint that imposes minimum latency requirements, these cyclic constraints often conflict with the target Π , making pipelined scheduling a notoriously difficult problem. Previously, ad hoc greedy heuristics have been proposed for different objectives and constraints (Cong & Zhang, 2006; Radivojevic & Brewer, 1996; Ku & De Micheli, 2002).

Differentiable Methods (Cai et al., 2025; Bengio et al., 2021; Lin et al., 2019) have recently emerged as a powerful alternative, bridging the gap between the speed of heuristics and the global search capabilities of exact solvers. By relaxing discrete scheduling decisions into continuous probabilistic distributions, these methods transform the combinatorial search space into a differentiable surface. This relaxation enables the use of first-order optimizers and GPU-accelerated vectorization to process massive amount of operators simultaneously. One primary advantage of this approach is its ability to handle complex, non-linear cost functions, such as memory footprint or learning based cost models (Chen et al., 2024; Wu et al., 2023), through smooth approximations that would be mathematically intractable for traditional solvers. Unlike greedy heuristics, differentiable methods provide a holistic, global view of the optimization landscape, allowing for the simultaneous optimization of all node assignments.

The first significant application of this paradigm to the scheduling domain was proposed in GS-Schedule (Liu et al., 2024). This approach models the probability of scheduling an operator to a specific step as a categorical distribution. To bridge the gap between continuous optimization and discrete execution, it utilizes the Gumbel-Softmax trick (Jang et al., 2016), which provides a differentiable way to sample from discrete distributions during optimization while

gradually annealing toward a discrete schedule.

3. Method

3.1. Gaussian Reparameterization

The previous differentiable scheduling attempt (Liu et al., 2024), represents the placement of an operator v_i as a categorical distribution over D discrete steps, which requires a parameter size of $D \cdot |V|$. Such a formulation suffers from two primary limitations:

Ordinal blindness: Categorical distributions treat steps as independent, nominal labels. From the optimizer’s perspective, the relationship between step d and $d + 1$ is mathematically identical to that between d and $d + 100$. This ignores the fundamental ordinal nature of time; in scheduling, proximity in the timeline should imply proximity in the optimization space.

Insufficient scalability: the optimization space $\mathbb{R}^{D \cdot |V|}$ becomes prohibitively large, as either maximum depth D or the number of operators $|V|$ increases. This limitation becomes increasingly prominent as the needs for large-scale modern workloads scheduling (Abts et al., 2020; Soi et al., 2025) increases.

To address these limitations, we propose **Gaussian reparameterization**. In stead of D categorical probabilities, we model the schedule of each operator v_i as an independent Gaussian random variable X_i :

$$X_i \sim \mathcal{N}(\mu_i, \sigma_i^2)$$

where $\mu_i \in \mathbb{R}$ represents the expected scheduling step and $\sigma_i \in \mathbb{R}^+$ represents the standard deviation of the distribution. The probability density function (PDF), $p(x; \mu_i, \sigma_i)$, represents the likelihood of an operator being scheduled at any continuous point x along the timeline. Figure 2 illustrates Gaussian reparameterization.

By adopting this parameterization, we reduce the number of parameters to be optimized from $D \cdot |V|$ to $2|V|$. For a graph with N operators, we only need to optimize two vectors: mean vector ($\boldsymbol{\mu} \in \mathbb{R}^{|V|}$) that determines the central temporal location of each operator, and standard deviation vector ($\boldsymbol{\sigma} \in \mathbb{R}^{|V|}$) that controls the degree of relaxation. During initial stage of optimization, $\boldsymbol{\sigma}$ is typically large to encourage exploration of the schedule space; as optimization processes, $\boldsymbol{\sigma}$ usually converges to small values concentrating the probability mass and effectively hardening the schedule toward a deterministic discrete integer.

This Gaussian relaxation also introduces a crucial **temporal inductive bias**. Because the Gaussian PDF $\phi(\mathbf{X}; \boldsymbol{\mu}, \boldsymbol{\sigma})$ is a continuous, unimodal function, updates to $\boldsymbol{\mu}$ produce a smooth gradient signal that pulls the operator through adjacent steps. This prevents the vanishing gradient prob-

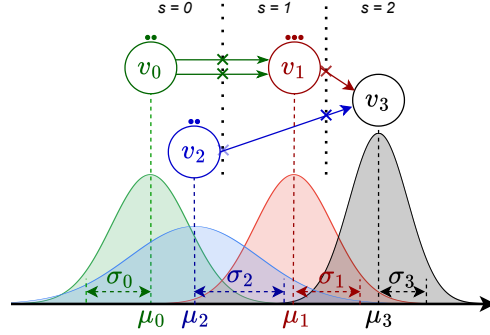


Figure 2. **Illustration of Gaussian reparameterization** — Each operator v_i is parameterized as an independent continuous random variable $X_i \sim \mathcal{N}(\mu_i, \sigma_i^2)$ over the scheduling timeline. The means μ_i represents the expected execution step, while the standard deviation σ_i reflects the uncertainty level.

lem common in categorical formulations, where shifting probability mass across zero-valued buckets provides no informative signal to the optimizer.

3.2. Representing Objectives and Constraints

With the Gaussian reparameterization established, the scheduling optimization is transformed into minimizing the expectations of performance objectives and constraint violations with respect to the parameters $(\boldsymbol{\mu}, \boldsymbol{\sigma})$. By optimizing the expected values, we ensure that the continuous parameter space accurately reflects the costs of the discrete schedules sampled from it. We illustrate this through two important metrics used in regular scheduling; the full derivations, including pipelined scheduling, are provided in Appendix B.

As emphasized in (Lin et al., 2019; Liu et al., 2024; Cai et al., 2025), It is important to maintain consistency between optimization and the final sampling process for differentiable combinatorial optimization. In our framework, to extract a discrete schedule from continuous variables, we round X_i to the nearest integer. Therefore, we use probability P_i^d to represent operator v_i being scheduled at step d by integrating the Gaussian PDF over the unit interval centered at d , which is used to align the sampling and optimization:

$$P_i^d = P \{ \lfloor X_i + 0.5 \rfloor = d \} \quad (7a)$$

$$= \Phi \left(\frac{d + 0.5 - \mu_i}{\sigma_i} \right) - \Phi \left(\frac{d - 0.5 - \mu_i}{\sigma_i} \right) \quad (7b)$$

Here $\lfloor \cdot \rfloor$ denotes truncation and $\Phi(\cdot)$ is the standard Gaussian cumulative distribution function (CDF). This formulation is efficient and differentiable. Notably, the latency constraint (Lat) is implicitly enforced by bounding the range

Algorithm 1 GauS algorithm

Input: $G = (V, E)$, max depth D , initial mean μ_0
Parameters: Lagrange ratios ρ , std factor κ .

Initialization:

 Compute s^{ASAP} and s^{ALAP}

 Set $\sigma = \kappa \cdot (s^{ALAP} - s^{ASAP})$

 Set $\mu = \mu_0$
repeat

 Compute primary objectives $\widehat{\mathcal{L}}(\mu, \sigma)$

 Compute expected constraint violations $\widehat{\mathcal{V}}_i(\mu, \sigma), \forall i$

 Compute $\mathcal{L}_{total} = \widehat{\mathcal{L}} + \sum_i \left(\lambda_i \widehat{\mathcal{V}}_i + \frac{\rho}{2} \|\widehat{\mathcal{V}}_i\|^2 \right)$

 Update $\mu, \sigma \leftarrow \text{optimizer}(\nabla \mathcal{L}_{total})$

 Update $\lambda_i \leftarrow \lambda_i + \rho \widehat{\mathcal{V}}_i, \forall i$

 Discrete schedule $s = \text{round}(\mu)$
 $\mu, \sigma \leftarrow \text{legalize}(s)$ if s is illegal

until convergence or time limit exceed

Output: Discrete schedule $s = \text{round}(\mu)$.

of d within $\{0, \dots, D-1\}$ ². Given P_i^d , the expectation of global objectives and violations of constraints can be expressed as differentiable functions of μ and σ .

For *dependency constraint*, we calculate the expected number of violations across all edges. A violation occurs if a consumer v_j is scheduled at a step d_j that is earlier than the producer v_i 's step d_i . Thus the expected violations of dependency constraint $\widehat{\mathcal{V}}_{Dep}$ is

$$\widehat{\mathcal{V}}_{Dep} = \mathbb{E}[\mathcal{V}_{Dep}] \quad (8a)$$

$$= \sum_{(v_i, v_j) \in E} \sum_{d_i=1}^{D-1} \sum_{d_j=0}^{d_i-1} P_i^{d_i} \cdot P_j^{d_j} \quad (8b)$$

Memory footprint requires calculating the probability that an operator's output is active at step d . A storage unit for v_i is occupied if the operator has started ($X_i \leq d$) but at least one successor v_j has not yet been scheduled ($X_j > d$). The expected storage unit count at step d is:

$$\widehat{Reg}(d) = \mathbb{E}[Reg(d)] \quad (9a)$$

$$= \sum_{v_i \in V} P \left\{ X_i \leq d < \max_{v_j \in succ(v_i)} X_j \right\} \cdot b_i \quad (9b)$$

$$= \sum_{v_i \in V} \left(\sum_{d_i=0}^d P_i^{d_i} \right) \cdot \left(1 - \prod_{v_j \in succ(v_i)} \sum_{d_j=0}^d P_j^{d_j} \right) \cdot b_i \quad (9c)$$

The global memory footprint is defined by the max pressure across all steps. Since the `max` function is non-differentiable, we employ the `LogSumExp` operator as a

²The lower limit for the first step ($d = 0$) and the upper limit for the last step ($d = D-1$) are set to $-\infty$ and $+\infty$, respectively.

smooth, differentiable approximation for the expectation of `max`:

$$\widehat{\mathcal{L}}_{Reg} = \mathbb{E} \left[\max_s Reg(d) \right] \quad (10a)$$

$$\approx \tau \cdot \log \left(\sum_s \exp \left(\frac{\widehat{Reg}(d)}{\tau} \right) \right) \quad (10b)$$

The temperature parameter τ controls how closely `LogSumExp` approximates `max`.

3.3. Overall Algorithm

Optimization. By deriving the expected objectives and constraint violations, the discrete scheduling problem is transformed into a continuous constrained optimization problem. A naive approach would be to minimize a weighted sum of the primary objective ($\widehat{\mathcal{L}}$) and the penalty terms for violations of all constraints ($\widehat{\mathcal{V}}_i, \forall i$):

$$\min_{\mu, \sigma} \widehat{\mathcal{L}} + \sum_i \lambda_i \widehat{\mathcal{V}}_i \quad (11)$$

where λ_i are static regularization coefficients, \mathcal{L} and \mathcal{V}_i are functions of σ and μ . However, manually tuning λ_i to balance the trade-off between optimality and feasibility is often computationally prohibitive.

To overcome the limitations of static weighting, we employ *augmented Lagrangian method (ALM)* (Powell, 1969; Hestenes, 1969). ALM dynamically adapts the penalty coefficients based on the magnitude of violations, ensuring that constraints are enforced as optimization progresses. The objective function becomes:

$$\min_{\mu, \sigma} \mathcal{L}_{total} = \widehat{\mathcal{L}} + \sum_i \left(\lambda_i \widehat{\mathcal{V}}_i + \frac{\rho}{2} \|\widehat{\mathcal{V}}_i\|^2 \right) \quad (12)$$

where ρ is a global penalty parameter. Initially, λ_i is set to a negligible value (e.g., 10^{-6}). After each iteration, λ_i is updated according to the rule $\lambda \leftarrow \lambda_i + \rho \widehat{\mathcal{V}}_i$. This mechanism ensures that hard constraints receive increasing attention from the optimizer until they are fully satisfied.

Sampling. To sample a discrete schedule from the continuous representation, we round the mean (μ_i) for each operator (v_i) to its nearest integer. While ALM minimizes expected violations, the resulting rounded schedule may still contain legal conflicts. To ensure the final output is valid, we apply a lightweight greedy algorithm to map illegal schedules to the nearest feasible ones. These legalized schedules are then used to re-initialize the parameters (μ, σ) for further optimization (see Appendix A for detailed algorithm).

Initialization. A core strength of GauS is its ability to capture temporal proximity, which allows it to exploit informed initialization. Unlike categorical models that begin with a flat, uninformed distributions, GauS can center its

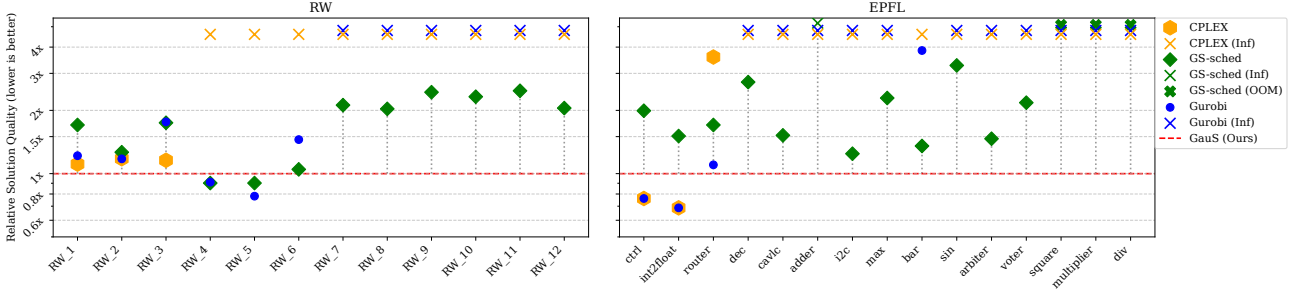


Figure 3. **Formulation A: Latency constrained, resource and communication optimization** — Problem instance size ($|V|$) increases from left to right. A 15-minute time limit is applied to all methods. Relative solution quality is represented as the ratio between the methods’ solution quality and GauS, where lower values correspond to higher solution quality. Light crosses (labeled as inf) denote no feasible solution or quality exceeding $4\times$ GauS performance; filled crosses indicate GS-Schedule exceeded available CUDA memory (OOM). On shared feasible instances, GauS achieves a **71.8%** geometric mean improvement over GS-Schedule.

search space around high-quality heuristics. For example, we can initialize the means μ as the output of list scheduling or at the midpoint of the ASAP and ALAP bounds: $\mu = (s^{ASAP} + s^{ALAP})/2$. For standard deviation σ , we initialize it proportional to the scheduling freedom of each node: $\sigma = \kappa \cdot (s^{ALAP} - s^{ASAP})$, where κ is a hyperparameter used to control the scale of the freedom.

To fully utilize the parallelism of modern GPUs, we vectorize the entire workflow. The complete algorithm for GauS is summarized in Algorithm 1.

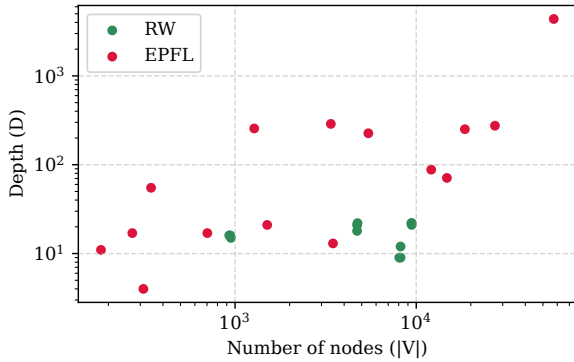


Figure 4. Overview of benchmark statistics.

4. Evaluation

4.1. Experimental Setup

To ensure a fair comparison, a 15-minute time limit is applied to all methods. Because GauS is deterministic given a fixed initialization, there is no variance between runs. Thus we report results from a single run per problem. We implement GauS in PyTorch and use A100 GPUs with 80 GB memory to run the experiments. More detailed settings are provided in Appendix C.1.

4.1.1. PROBLEM FORMULATIONS

Depending on the applications and context, scheduling problem may have different formulations (Lam, 1988; Cong & Zhang, 2006; Zhang & Liu, 2013). In the evaluation part, we will focus on three distinct formulations.

Formulation A: Latency-constrained, resources and communication optimization for regular scheduling. This formulation is used in GS-Schedule (Liu et al., 2024) which suits communication bottle-necked applications.

$$\min_s \mathcal{L}_{Res} + \alpha \mathcal{L}_{Com} \quad \text{s.t. } \underline{Dep}, \underline{Lat} \quad (13)$$

Here \mathcal{L}_{Com} represents an auxiliary communication overhead described in Appendix B.1, and α is an application-specific constant that balances the tradeoff between resources and communication, $s \in \mathbb{N}^n$ is vector form of $s_i, i \in \{0, \dots, n-1\}$.

Formulation B: Latency-constrained, memory footprint optimization for regular scheduling. In some realistic hardware workloads (Amarú et al., 2015), the peak storage units is more important:

$$\min_s \mathcal{L}_{Mem} \quad \text{s.t. } \underline{Dep}, \underline{Lat} \quad (14)$$

Formulation C: Latency, resources, and recurrence-constrained, memory footprint optimization for modulo scheduling. To further demonstrate the flexibility and understand performance of the schedulers, we also use modulo scheduling (Rau & Glaeser, 1981; Lam, 1988; Soi et al., 2025). For a given resources limit C_{res} , and given II:

$$\min_s \mathcal{L}_{MMem} \quad (15a)$$

$$\text{s.t. } \mathcal{L}_{MRes} \leq C_{Res}, \underline{Dep}, \underline{Lat}, \underline{Rec} \quad (15b)$$

4.1.2. BENCHMARKS

Due to the lack of publicly available large-scale scheduling datasets, we adopt and extend the benchmarks established

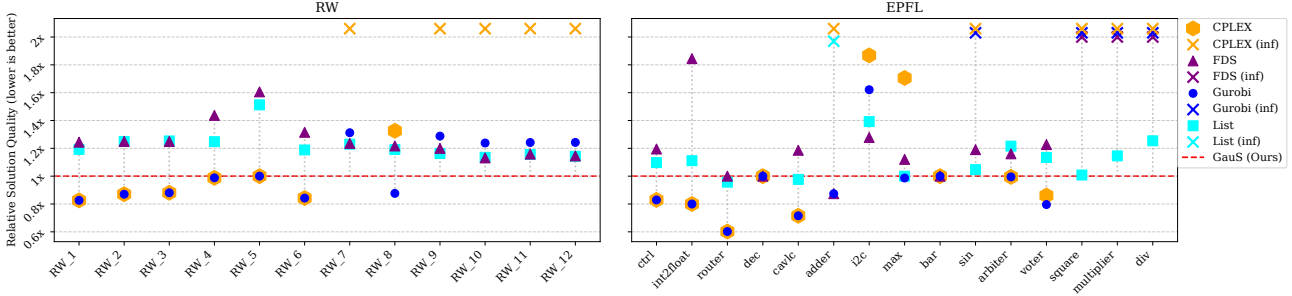


Figure 5. **Formulation B:** Latency constrained, memory footprint optimization — A 15-minute time limit is applied to all methods. Light crosses denote no feasible solution or quality exceeding $4\times$ GauS performance.

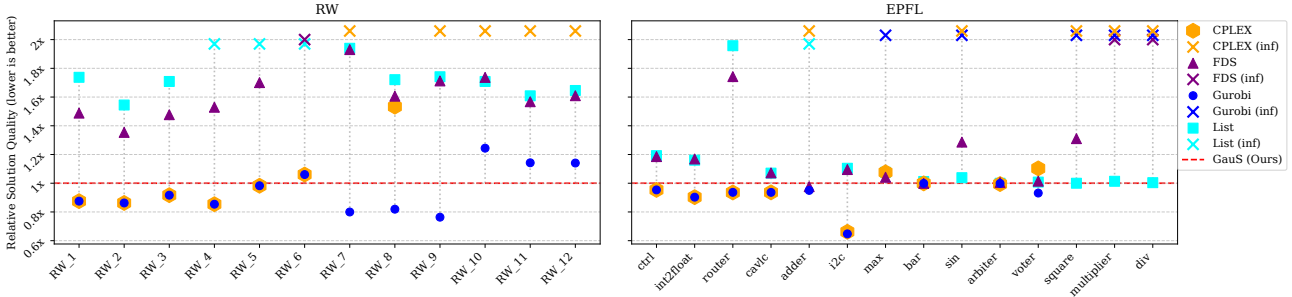


Figure 6. **Formulation C:** Latency, resources, and recurrence-constrained, memory footprint modulo optimization — A 15-minute time limit is applied to all methods. Light crosses denote no feasible solution or quality exceeding $4\times$ GauS performance. dec in EPFL has no feasible solution, thus omitted from the plot.

in recent literature (Liu et al., 2024). For unpipelined formulations (A and B), we evaluate GauS using the same suite as (Liu et al., 2024), which includes realistic workloads from the EPFL Benchmark Suites (Amarú et al., 2015) and synthetic random workloads (RW).

For the pipelined formulation C, existing benchmarks (Zhang & Liu, 2013; Oppermann et al., 2019) are too small for modern requirements. Thus, we synthesized new benchmarks by augmenting the EPFL and RW suites with resource and recurrence constraints, with the number of added recurrences proportionally to graph size. The overview of problem size is shown in Figure 4. More details can be found in Appendix C.2.

4.1.3. BASELINES

Exact Solvers. To understand the tradeoff on the quality spectrum, we use the state-of-the-art SDC+LP formulation (Cong & Zhang, 2006; Zhang & Liu, 2013) with the commercial solvers CPLEX (Bliek1ú et al., 2014) and Gurobi (Gurobi Optimization, LLC, 2023) as baselines.

Heuristics. To further understand the tradeoff on the speed spectrum, we also compare our methods with two popular heuristics: List Scheduling (Parker et al., 1986; Kondratyev et al., 2011) and Force-Directed Scheduling (FDS) (Verhaegh et al., 1992; Paulin & Knight, 1987).

Differentiable method. We compare to GS-Schedule only on formulation A, because this is the original formulation used in their work and is not straightforward to extend GS-Schedule to other formulation.

4.2. Quality Comparison

Formulation A: The quality comparison between GauS and traditional combinatorial solvers (CPLEX, Gurobi) as well as GS-Schedule is illustrated in Figure 3. The benchmarks are ordered by operator count ($|V|$) from left to right.

For smaller benchmarks, traditional ILP solvers often find optimal or near-optimal solutions. As the problem scale increases, GauS consistently produces high-quality schedules within the 15-minute time limit. In contrast, traditional solvers marked with light crosses fail to produce a feasible solution or result in a schedule quality exceeding $4\times$ the performance threshold relative to GauS.

While GS-Schedule is able to produce solutions on most benchmarks, the solution quality is about 30% to $3\times$ worse compared to GauS with a geometric mean of 71.8%. This demonstrates the superior efficacy of GauS. The memory efficiency reflects the other advantage of Gaussian reparameterization, parameter efficiency. As shown in the EPFL benchmarks, the GS-Schedule baseline frequently exceeds available CUDA memory (OOM) on larger graphs (repre-

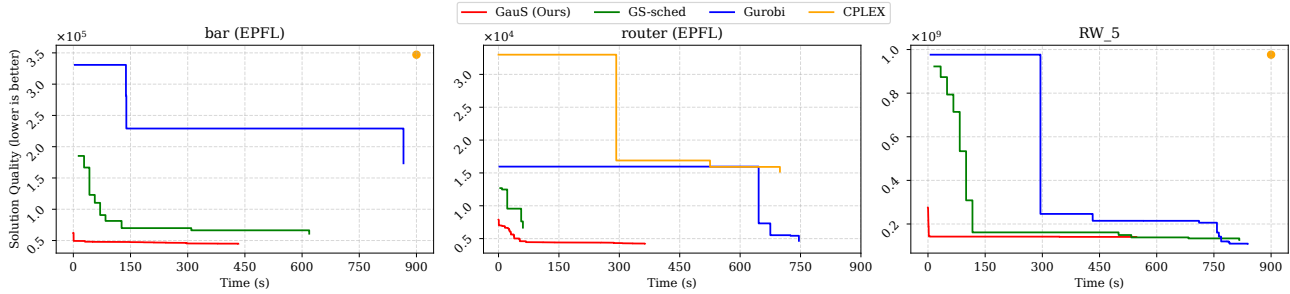


Figure 7. **Quality-Speed tradeoff representative benchmarks** – From left to right: RW_5, router, and bar on formulation A. Lines terminating before the 15-minute indicate no further improvement is made.

sented by filled cross markers), while GauS is able to produce solutions for large graphs. This parameter explosion is a direct consequence of their $O(ND)$ parameter space, whereas GauS maintains a linear parameter space, enabling the optimization of massive-scale designs that are physically untreatable by previous differentiable methods.

Formulation B and C: To demonstrate the versatility of GauS, we evaluate its performance on two advanced scheduling formulations: *latency-constrained, memory footprint optimization* and *latency, resource, and recurrence-constrained modulo optimization*.

While exact solvers like CPLEX and Gurobi achieve competitive results on smaller graphs, their performance degrades as problem scale increases, frequently exceeding the 15-minute time limit or failing to produce any feasible solution (indicated by light crosses). In contrast, GauS maintains a robust and stable performance profile, consistently matching or exceeding the quality of standard heuristics such as List Scheduling and Force-Directed Scheduling (FDS). On most benchmarks, these heuristics often result in 20% to 60% higher memory footprint than our method.

The performance gap narrows in large graphs in formulation C on EPFL. As the number of augmented back-edges is proportional to the graph size, feasible search space is significantly restricted, especially for large graphs. decreasing the overall degrees of freedom, making the margin for potential improvement becomes inherently smaller.

4.3. Tradeoff Analysis

To evaluate optimization efficiency, we analyze the any-time results (solution quality vs. runtime) for GauS against baselines. Figure 7 illustrates tradeoff for a subset of problems in Formulation A, with comprehensive results for all benchmarks provided in Appendix E.

GauS consistently reaches high-quality solutions significantly faster than all baselines including GS-Schedule and commercial solvers, even for RW_5 where the eventual solution slightly falls short. When both methods eventually

converge to similar objectives, GauS achieves equivalent solution quality one to two orders of magnitude faster. The results shows that GauS achieves Pareto-optimal results.

Furthermore, GauS significantly enhances the utilization of GPU parallelism as detailed in Appendix D. While GS-Schedule drops below 40% on averaged GPU utilization as complexity increases, GauS maintains near-100%.

5. Conclusion

In this work, we presented GauS, a scalable differentiable framework for operator scheduling designed to overcome the bottlenecks of traditional combinatorial solvers and categorical differentiable models. By leveraging a Gaussian reparameterization, GauS achieves $O(|V|)$ parameter scalability, enabling the optimization of massive-scale hardware designs with tens of thousands of nodes that were previously considered intractable. As the first differentiable method to support pipelined scheduling, GauS offers a unique level of flexibility. Our experimental results across realistic and synthetic workloads demonstrate that GauS delivers the state-of-the-art convergence speeds and high-quality solutions, making it as a robust tool for modern scheduling problem.

Despite its scalability, the current framework may occasionally converge to suboptimal solutions. This is partly due to the modeling of operators as independent Gaussian variables, which neglects interactions between nodes, particularly those sharing the same edge. While a Gaussian Process could capture these correlations, it introduces a prohibitive $O(|V|^2)$ space complexity. Future work could explore more efficient ways to model node correlations and investigate advanced optimization strategies to further enhance convergence stability and solution quality.

Impact Statement

GauS focuses on the scalability bottleneck in operator scheduling, enabling the efficient optimization of designs with tens of thousands of nodes, potentially contributing to the creation of higher-performance, energy-efficient computing systems for large-scale industrial applications

References

- Abts, D., Ross, J., Sparling, J., Wong-VanHaren, M., Baker, M., Hawkins, T., Bell, A., Thompson, J., Kahsai, T., Kimmell, G., et al. Think fast: A tensor streaming processor (tsp) for accelerating deep learning workloads. In *2020 ACM/IEEE 47th Annual International Symposium on Computer Architecture (ISCA)*, pp. 145–158. IEEE, 2020.
- Amarú, L., Gaillardon, P.-E., and De Micheli, G. The eplf combinational benchmark suite. *Hypotenuse*, 256(128): 214335, 2015.
- Bengio, Y., Lodi, A., and Prouvost, A. Machine learning for combinatorial optimization: a methodological tour d’horizon. *European Journal of Operational Research*, 290(2):405–421, 2021.
- Blikelú, C., Bonami, P., and Lodi, A. Solving mixed-integer quadratic programming problems with ibm-cplex: a progress report. *Proceedings of the twenty-sixth RAMP symposium*, pp. 16–17, 2014.
- Cai, Y., Yang, K., Deng, C., Yu, C., and Zhang, Z. Smoother: Differentiable e-graph extraction. In *Proceedings of the 30th ACM International Conference on Architectural Support for Programming Languages and Operating Systems, Volume 1*, pp. 1020–1034, 2025.
- Chen, C., Hu, G., Zuo, D., Yu, C., Ma, Y., and Zhang, H. E-syn: E-graph rewriting with technology-aware cost functions for logic synthesis. In *Proceedings of the 61st ACM/IEEE Design Automation Conference*, pp. 1–6, 2024.
- Cong, J. and Zhang, Z. An efficient and versatile scheduling algorithm based on sdc formulation. In *Proceedings of the 43rd annual Design Automation Conference*, pp. 433–438, 2006.
- Fan, K., Kudlur, M., Park, H., and Mahlke, S. Cost sensitive modulo scheduling in a loop accelerator synthesis system. In *38th Annual IEEE/ACM International Symposium on Microarchitecture (MICRO’05)*, pp. 12–pp. IEEE, 2005.
- Fan, K., Park, H. h., Kudlur, M., and Mahlke, S. o. Modulo scheduling for highly customized datapaths to increase hardware reusability. In *Proceedings of the 6th annual IEEE/ACM international symposium on Code generation and optimization*, pp. 124–133, 2008.
- Gebotys, C. and Elmasry, M. Global optimization approach for architectural synthesis. *IEEE Transactions on Computer-Aided Design of Integrated Circuits and Systems*, 12(9):1266–1278, 1993. doi: 10.1109/43.240074.
- Guo, D., Gholamrezaei, M., Hofmann, M., Venkat, A., Zhang, Z., and Skadron, K. Pimsynth: A unified compiler framework for bit-serial processing-in-memory architectures. *IEEE Computer Architecture Letters*, 2025.
- Gurobi Optimization, LLC. Gurobi Optimizer Reference Manual, 2023. URL <https://www.gurobi.com>.
- Hestenes, M. R. Multiplier and gradient methods. *Journal of optimization theory and applications*, 4(5):303–320, 1969.
- Hwang, C.-T., Lee, J.-H., and Hsu, Y.-C. A formal approach to the scheduling problem in high level synthesis. *IEEE Transactions on Computer-Aided Design of Integrated Circuits and Systems*, 10(4):464–475, 2002.
- Jang, E., Gu, S., and Poole, B. Categorical reparameterization with gumbel-softmax. *arXiv preprint arXiv:1611.01144*, 2016.
- Kondratyev, A., Lavagno, L., Meyer, M., and Watanabe, Y. Realistic performance-constrained pipelining in high-level synthesis. In *2011 Design, Automation & Test in Europe*, pp. 1–6. IEEE, 2011.
- Ku, D. C. and De Micheli, G. Relative scheduling under timing constraints: Algorithms for high-level synthesis of digital circuits. *IEEE Transactions on Computer-Aided Design of Integrated Circuits and Systems*, 11(6):696–718, 2002.
- Lam, M. Software pipelining: An effective scheduling technique for vliw machines. In *Proceedings of the ACM SIGPLAN 1988 conference on Programming Language design and Implementation*, pp. 318–328, 1988.
- Leiserson, C. E. and Saxe, J. B. Retiming synchronous circuitry. *Algorithmica*, 6(1):5–35, 1991.
- Lin, Y., Dhar, S., Li, W., Ren, H., Khailany, B., and Pan, D. Z. Dreamplace: Deep learning toolkit-enabled gpu acceleration for modern vlsi placement. In *Proceedings of the 56th Annual Design Automation Conference 2019*, pp. 1–6, 2019.
- Liu, M., Li, Y., Yin, J., Zhang, Z., and Yu, C. Differentiable combinatorial scheduling at scale. In *Proceedings of the 41st International Conference on Machine Learning*, pp. 31464–31476, 2024.

- Oppermann, J., Reuter-Oppermann, M., Sommer, L., Koch, A., and Sinnen, O. Exact and practical modulo scheduling for high-level synthesis. *ACM Transactions on Reconfigurable Technology and Systems (TRETS)*, 12(2):1–26, 2019.
- Parker, A. C., Pizarro, J., and Mlinar, M. Maha: A program for datapath synthesis. In *23rd ACM/IEEE Design Automation Conference*, pp. 461–466. IEEE, 1986.
- Paulin, P. G. and Knight, J. P. Force-directed scheduling in automatic data path synthesis. In *Proceedings of the 24th ACM/IEEE Design Automation Conference, DAC '87*, pp. 195–202, New York, NY, USA, 1987. Association for Computing Machinery. ISBN 0818607815. doi: 10.1145/37888.37918. URL <https://doi.org/10.1145/37888.37918>.
- Powell, M. J. A method for nonlinear constraints in minimization problems. *Optimization*, pp. 283–298, 1969.
- Radivojevic, I. and Brewer, F. A new symbolic technique for control-dependent scheduling. *IEEE transactions on computer-aided design of integrated circuits and systems*, 15(1):45–57, 1996.
- Rau, B. R. and Glaeser, C. D. Some scheduling techniques and an easily schedulable horizontal architecture for high performance scientific computing. *ACM SIGMICRO Newsletter*, 12(4):183–198, 1981.
- Seshadri, V., Lee, D., Mullins, T., Hassan, H., Boroumand, A., Kim, J., Kozuch, M. A., Mutlu, O., Gibbons, P. B., and Mowry, T. C. Ambit: In-memory accelerator for bulk bitwise operations using commodity dram technology. In *Proceedings of the 50th Annual IEEE/ACM International Symposium on Microarchitecture*, pp. 273–287, 2017.
- Soi, R., Yadav, R., Kjolstad, F., Aiken, A., Dehnavi, M. M., Garland, M., and Bauer, M. Optimal software pipelining and warp specialization for tensor core gpus. *arXiv preprint arXiv:2512.18134*, 2025.
- Verhaegh, Lippens, Aarts, Korst, van der Werf, and van Meerbergen. Efficiency improvements for force-directed scheduling. In *1992 IEEE/ACM International Conference on Computer-Aided Design*, pp. 286–291, 1992. doi: 10.1109/ICCAD.1992.279359.
- Wu, N., Li, Y., Hao, C., Dai, S., Yu, C., and Xie, Y. Gamora: Graph learning based symbolic reasoning for large-scale boolean networks. In *2023 60th ACM/IEEE Design Automation Conference (DAC)*, pp. 1–6. IEEE, 2023.
- Zhang, H., Li, D., and Shen, H. A sat based scheduler for tournament schedules. In *SAT*, 2004.
- Zhang, N., Agnesina, A., Shbat, N., Leader, Y., Zhang, Z., and Ren, H. Cypress: Vlsi-inspired pcb placement with gpu acceleration. In *Proceedings of the 2025 International Symposium on Physical Design*, pp. 31–41, 2025.
- Zhang, Y., Ren, H., Sridharan, A., and Khailany, B. Gatspi: Gpu accelerated gate-level simulation for power improvement. In *Proceedings of the 59th ACM/IEEE Design Automation Conference*, pp. 1231–1236, 2022.
- Zhang, Z. and Liu, B. Sdc-based modulo scheduling for pipeline synthesis. In *2013 IEEE/ACM International Conference on Computer-Aided Design (ICCAD)*, pp. 211–218. IEEE, 2013.

A. Legalization Heuristic

While the Gaussian stochastic relaxation encourages valid schedules through dependency penalties, rounding learned means μ_i to discrete integers s_i can occasionally result in causality violations. Therefore, we use some heuristics to legalize any solution that violates the constraint. Because of the recurrence constraint in modulo scheduling, we use two different legalization heuristic for regular and modulo scheduling problem.

A.1. Regular Scheduling Legalization Heuristic

To ensure strict feasibility, we employ a topological legalization pass. This procedure processes the graph in topological order, shifting nodes forward in time only when necessary to satisfy dependency latencies while remaining within the pre-defined ASAP and ALAP bounds. By performing this one-pass refinement, we try to legalize the discrete output without significantly altering the global optimization results. The algorithm is summarized in Algorithm 2

Algorithm 2 Regular Schedule Legalization

Input: $G = (V, E)$, rounded schedule s .
 Compute s^{ASAP} and s^{ALAP}
 $s_{new} \leftarrow \text{clamp}(s, \min = s^{ASAP}, \max = s^{ALAP})$
for each node v in `topological_sort(G)` **do**
 $preds \leftarrow \{v_j \mid (v_j, v) \in E\}$
 if $|preds| > 0$ **then**
 $t_{req} \leftarrow \max(s_{new}[Preds]) + 1$
 $s_{new}[v] \leftarrow \max(s_{new}[v], t_{req})$
 end if
end for
Output: Feasible discrete schedule s_{new} .

A.2. Modulo Scheduling Legalization Heuristic

Modulo scheduling introduces cyclic constraints due to back-edges. To resolve these, we employ a simple fixed-point relaxation algorithm. Unlike standard topological legalization, this iterative approach repeatedly passes through the graph to resolve back-edge requirements alongside forward dependencies. The process continues until the schedule stabilizes or a maximum iteration threshold (equal to the number of nodes) is reached, signaling a potential recurrence violation or depth overflow. This tries to find a feasible schedule for pipelined execution while not significantly changing the original input. The algorithm is summarized in Algorithm 3.

B. Derivations

We finish the derivation of expected objectives and violations of constraints in this section. After defining communication overhead, we will compute its expectation and expected resource usage under regular scheduling before deriving the metrics essential to modulo scheduling

B.1. Communication overhead

In communication-bottlenecked workloads (Zhang et al., 2022), we minimize the total edge length across all dependencies:

$$\mathcal{L}_{Com} = \sum_{(v_i, v_j) \in E} s_j - s_i \quad (16)$$

Then the expected total edge length $\widehat{\mathcal{L}}_{Com}$ is the sum of all expected violations from all edges:

$$\widehat{\mathcal{L}}_{Com} = \mathbb{E}[\mathcal{L}_{Com}] = \sum_{(v_i, v_j) \in E} \sum_{d_i=0}^{D-1} \sum_{d_j=d_i}^{D-1} P_i^{d_i} P_j^{d_j} \cdot (d_j - d_i) \quad (17)$$

Algorithm 3 Modulo Schedule Legalization

Input: $G = (V, E)$, back-edge set E_B , max depth D , initiation interval Π , rounded schedule s .

```

 $s_{new} \leftarrow s$ 
 $nodes \leftarrow \text{topological\_sort}(G)$ 
for  $i = 0$  to  $|V| - 1$  do
     $changed \leftarrow \text{False}$ 
    for each  $v$  in  $nodes$  do
         $t_{min} \leftarrow \max(\{s_{new}[u] \mid u \in \text{preds}(v)\} \cup \{0\}) + 1$ 
         $t_{back} \leftarrow \max(\{s_{new}[v_j] - k \cdot \Pi + 1 \mid (v, v_j, k) \in E_B\} \cup \{0\})$ 
         $t_{req} \leftarrow \max(t_{min}, t_{back})$ 
        if  $t_{req} > s_{new}[v]$  then
             $s_{new}[v] \leftarrow t_{req}$ ,  $changed \leftarrow \text{True}$ 
        end if
    end for
    if not changed then
        break
    end if
end for
Output:  $s_{new}$ .
    
```

B.2. Expected Resource Usage

To represent the expected resource usage at step d , we reuse the probability that an operator v_i with resource demand w_i is active at that step defined in Equation 7. The expected resource usage is the sum of individual usage:

$$\widehat{Res}(d) = \mathbb{E}[Res(d)] = \sum_{v_i \in V} w_i \cdot P_i^d \quad (18)$$

To optimize for peak resource utilization, we apply the `LogSumExp` operator across all steps $d \in \{0, \dots, D - 1\}$. This is similar to the computation of global memory footprint in 3.2:

$$\widehat{\mathcal{L}}_{Res} \approx \tau \cdot \log \left(\sum_d \exp \left(\frac{\widehat{Res}(d)}{\tau} \right) \right) \quad (19)$$

We define the violations as the number of exceeded resources used summed across all steps. Then the expected violations can be computed as:

$$\widehat{\mathcal{V}}_{Res} = \sum_d \text{ReLU} \left(\widehat{Res}(d) - R \right) \quad (20)$$

where R is a given resources limit, and $\text{ReLU}(\cdot)$ ensures only exceeding resources are counted toward violations.

B.3. Modulo Metrics

In a pipeline, an operator scheduled at step d_i consumes resources at steps $d_i \bmod \Pi$. The probability that operator v_i occupies a resource at time $t \in \{0, \dots, \Pi - 1\}$ within the modulo reservation table is the sum of its probabilities across all linear steps that map to t :

$$P \{ \lfloor X_i + 0.5 \rfloor = t \} = \sum_{k=0}^{\lceil D/\Pi \rceil} P_i^{t+k \cdot \Pi} \quad (21)$$

where $P_i^{t+k \cdot \Pi}$ represents the probability of scheduling operator v_i to step $d = t + k \cdot \Pi$ is defined in Equation 7b.

Modulo Resource Usage. Similar to the derivation in 3.2, at step $0 \leq t < \Pi$, the expected modulo resource usage $\widehat{MRes}(t)$:

$$\widehat{MRes}(t) = \sum_{v_i \in V} w_i \cdot P \{ \lfloor X_i + 0.5 \rfloor = t \} \quad (22)$$

Modulo Memory Footprint. Memory footprint in a pipeline is similarly wrapped. A memory unit carrying the output of v_i is active at step t if it is active at any time step d such that $d = t + k \cdot \Pi, k > 0$. Using the linear probability $P(X_i \leq s < \max_{v_j \in \text{succ}(v_i)} X_j)$ defined in Equation 9b, we can compute the modulo expectation:

$$\widehat{MReg}(t) = \sum_{v_i \in V} b_i \cdot \sum_{k=0}^{\lceil D/\Pi \rceil} P \left\{ d_i \leq t + k \cdot \Pi < \max_{v_j \in \text{succ}(i)} d_j \right\} \quad (23)$$

The expected maximum modulo resource usage and peak memory footprint can be computed using `LogSumExp` similar to Equation 10b. The expected violations can be computed using `ReLU` similar to Equation 20.

Recurrence Violations. For modulo scheduling with loop-carried dependencies, a back-edge from producer v_j to consumer v_i with an iteration distance k and latency $\text{Lat}(v_i)$ imposes the constraint $s_i + k \cdot \Pi \geq s_j + \text{Lat}(v_i)$. Let the set of these dependencies be defined as $(v_j, v_i, k) \in E_B$. Similar to the computation of expected dependency violations in Equation 8, the expected recurrence violation \widehat{V}_{rec} is formulated by summing the probabilities of all invalid steps assignments (d_i, d_j) that fail to satisfy the recurrence constraint:

$$\widehat{V}_{Rec} = \mathbb{E}[V_{Rec}] = \sum_{(v_i, v_j, k) \in E_B} \sum_{d_i=1}^{D-1} \sum_{d_j=d_i+k \cdot \Pi+1}^{D-1} P_i^{d_i} \cdot P_j^{d_j} \quad (24)$$

C. Detailed Evaluation Setup

C.1. Experiment Setup

Environment Settings. All the experiments are performed on a Linux server equipped two NVIDIA A100 GPUs with 80 GB memory and two AMD EPYC 9124 CPUs (2×16 cores) running at 3.7 GHz, 1.5 TB of RAM. For softwares, we use PyTorch 2.5.1 with CUDA 12.1, Gurobi 13.0, and CPLEX 22.1.1.

Hyper-parameter Settings. We use a uniform set of hyperparameters across all problem instances and formulations. We use the Adam optimizer with a learning rate of 10^{-2} . The penalty parameter ρ , used to enforce constraints, is set to 10^{-4} ; the `LogSumExp` temperature parameter τ is set to 10^{-2} ; the initialization freedom parameter κ is set to $\frac{1}{6}$.

C.2. Dataset Details

For the random workload (RW) evaluations, we utilize a subset of the datasets released by GS-Schedule (Liu et al., 2024), though our selected subset is substantially larger than the one featured in the original study to better evaluate scalability.

D. GPU Efficiency Analysis

To evaluate the practical GPU efficiency of GauS, we performed a comparative GPU profiling analysis against the baseline, GS-Schedule, using the EPFL benchmarks. Figure 8 illustrates the peak GPU memory usage and compute utilization across various workloads.

Memory Scalability: GauS exhibits a remarkably consistent and relatively low memory footprint across all benchmarks, roughly linear with the size of the graph ($|V|$). In contrast, GS-Schedule shows a more drastic growth in memory consumption as the size ($|V|$) and the depth (D) of the graph increases, resulting out-of-memory (OOM) issues on the largest designs like square, multiplier, and div.

Compute Utilization: Our Gaussian parameterization consistently maintains near-100% averaged GPU utilization. This demonstrates that the $O(N)$ parameter space is not only memory-efficient but also highly amenable to parallel execution. Conversely, GS-Schedule struggles to saturate the GPU, with utilization dropping below 40% as the graph complexity increases, likely due their poor GPU implementation.

Table 1. Summary of Graph Statistics (Sorted by Nodes)

| EPFL | | | Random Workloads (RW) | | |
|------------|---------------------------|---------------|-----------------------|---------------------------|---------------|
| Name | Number of Nodes ($ V $) | Depth (D) | Name | Number of Nodes ($ V $) | Depth (D) |
| ctrl | 182 | 11 | RW_1 | 929 | 16 |
| int2float | 271 | 17 | RW_2 | 941 | 16 |
| dec | 312 | 4 | RW_3 | 949 | 15 |
| router | 344 | 55 | RW_4 | 4713 | 18 |
| cavlc | 703 | 17 | RW_5 | 4716 | 21 |
| adder | 1276 | 256 | RW_6 | 4741 | 22 |
| i2c | 1504 | 21 | RW_7 | 8058 | 9 |
| max | 3377 | 288 | RW_8 | 8192 | 12 |
| bar | 3471 | 13 | RW_9 | 8193 | 9 |
| sin | 5440 | 226 | RW_10 | 9396 | 22 |
| arbiter | 12095 | 88 | RW_11 | 9432 | 21 |
| voter | 14759 | 71 | RW_12 | 9447 | 22 |
| square | 18550 | 251 | | | |
| multiplier | 27190 | 275 | | | |
| div | 57375 | 4373 | | | |

E. Full Tradeoff Results

E.1. Formulation A

The full tradeoff analysis on formulation A is shown in Figure 9 and 10, GauS is on the Pareto frontier for most of the problem workloads, especially larger ones.

E.2. Formulation B and C

The comprehensive tradeoff results on formulation B and C are shown in Figure 11, 12, 13 and 14. The results demonstrate that while exact solvers like CPLEX and Gurobi achieve high-quality solutions for smaller problem instances, GauS is better in scalability, delivering good solutions on large-scale benchmarks. For medium-sized cases, our method offers a highly competitive tradeoff, reaching high-quality solutions orders of magnitude faster than exact solvers. Furthermore, GauS consistently outperforms fast heuristics, such as List Scheduling and FDS, which often usually leads to suboptimal results.

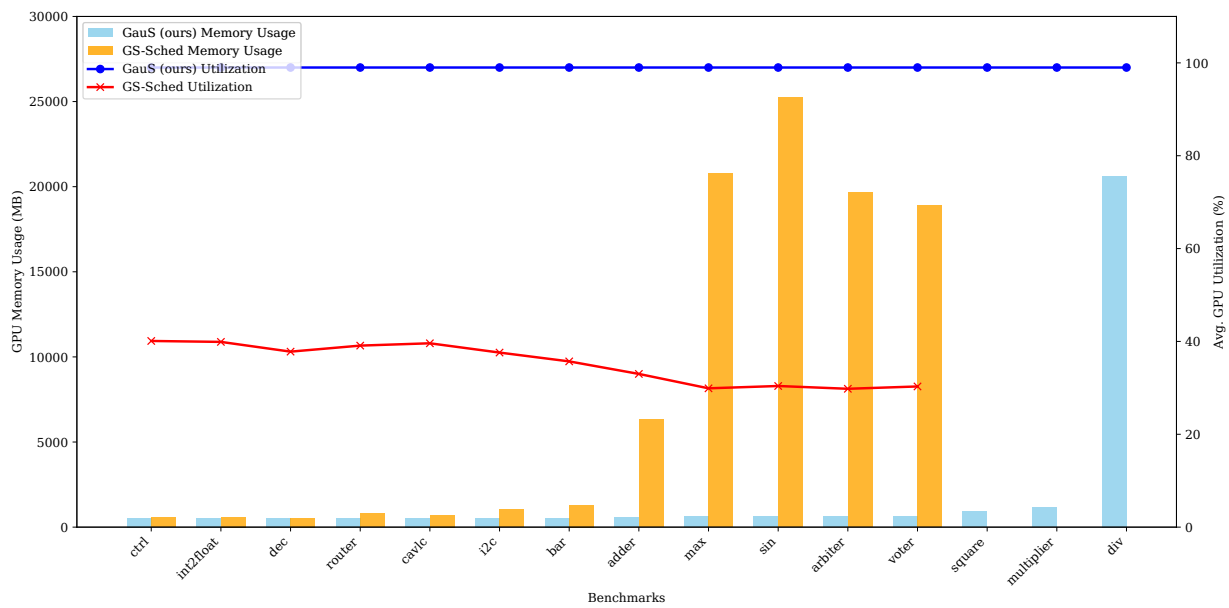


Figure 8. GPU Profiling Results on EPFL — The bar charts show the GPU memory usage, corresponding to the left axis. The curve show the Avg. GPU utilization, corresponding to the right axis. Avg. GPU utilization is the averaged GPU utilization (%) during the entire execution. Because GS-Schedule is out-of-memory (OOM) on square, multiplier, and div, no data is provided for GS-Schedule on these benchmarks

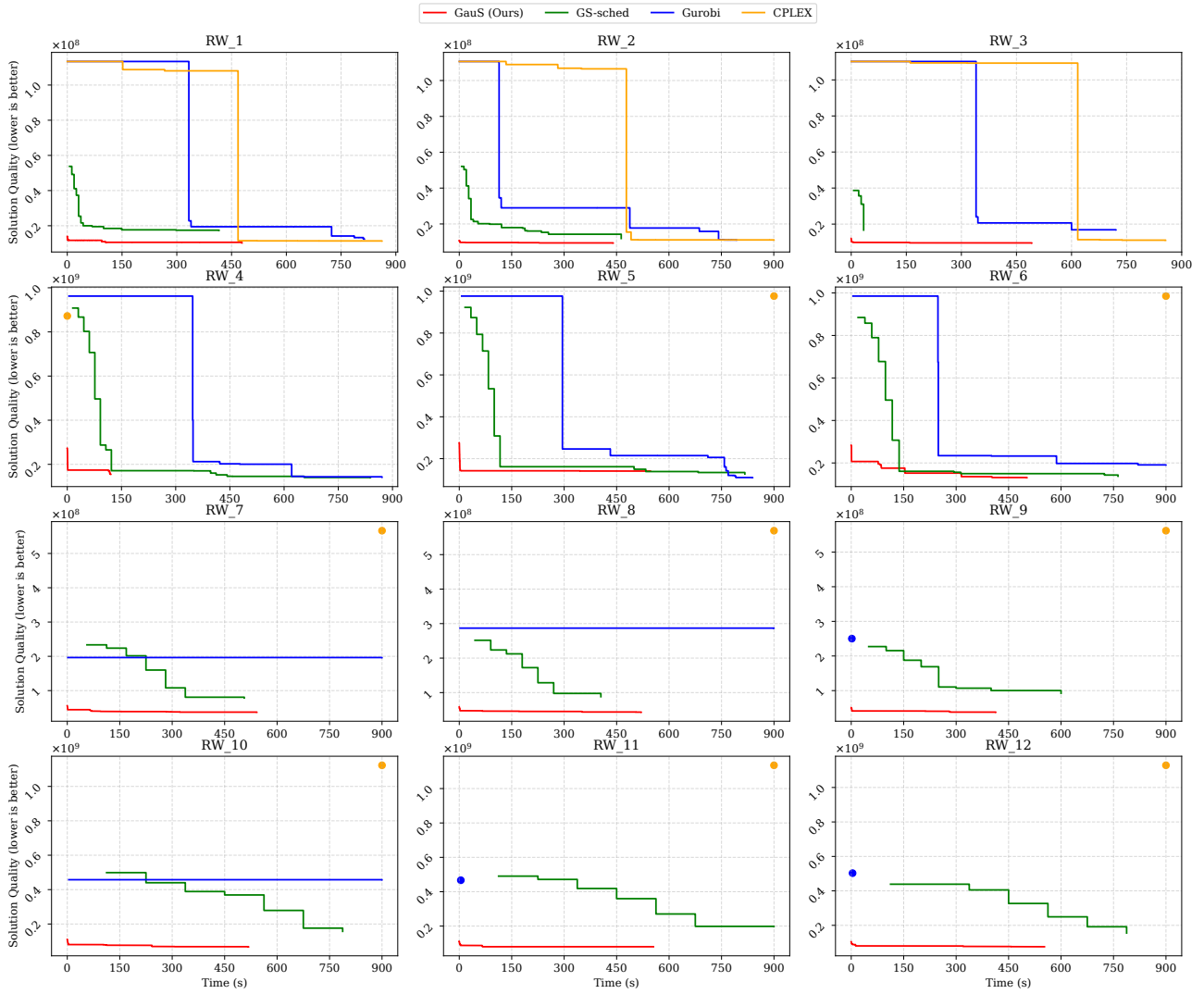


Figure 9. Comprehensive tradeoff comparison of RW on **Formulation B**: Latency constrained, resource and communication optimization — A 15-minute time limit is applied to all methods. Heuristics such as FDS and List Scheduling are represented as horizontal lines to reflect their fast convergence to final solution quality.

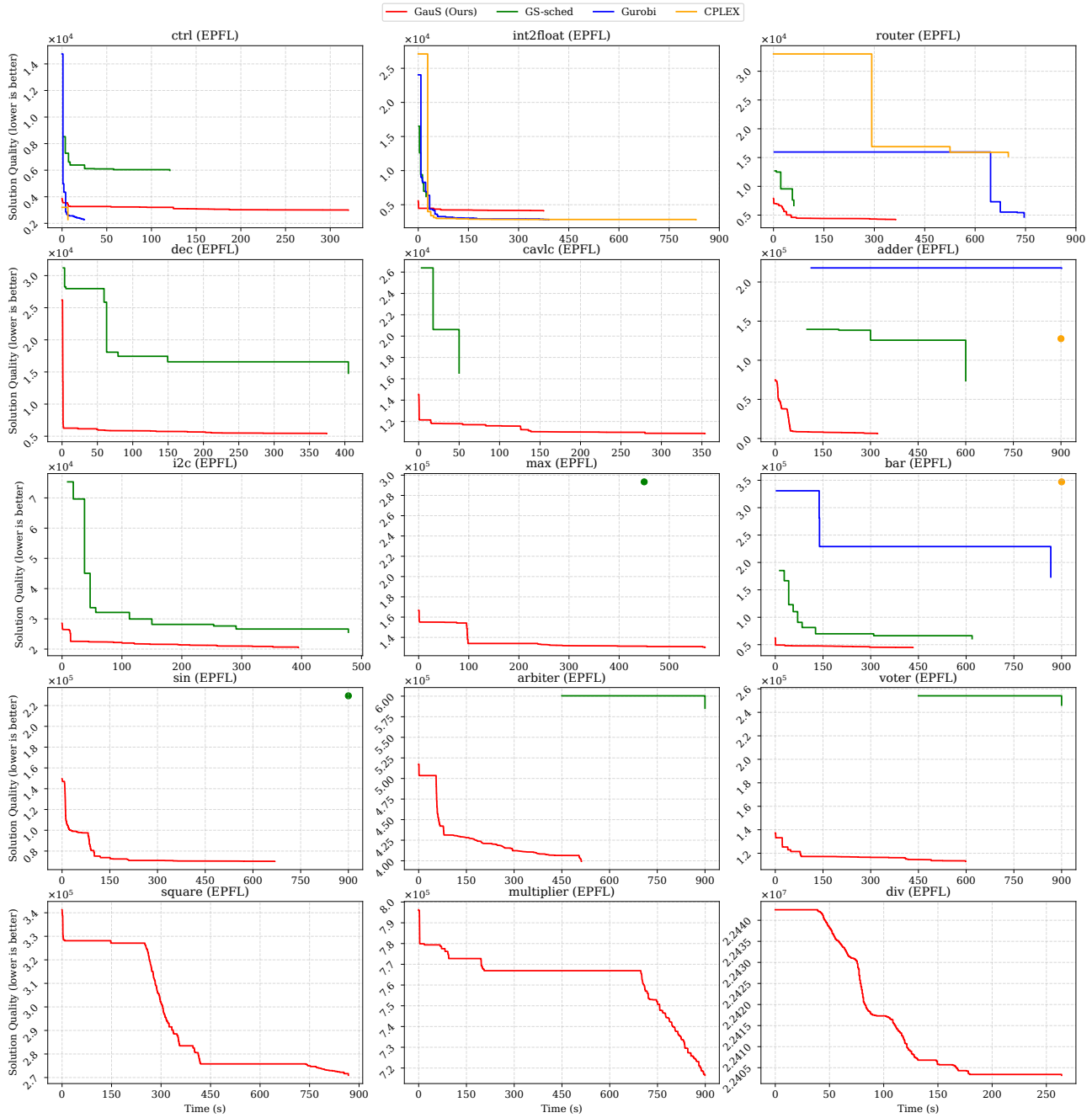


Figure 10. Comprehensive tradeoff comparison of EPFL on **Formulation A**: Latency constrained, resource and communication optimization — A 15-minute time limit is applied to all methods.

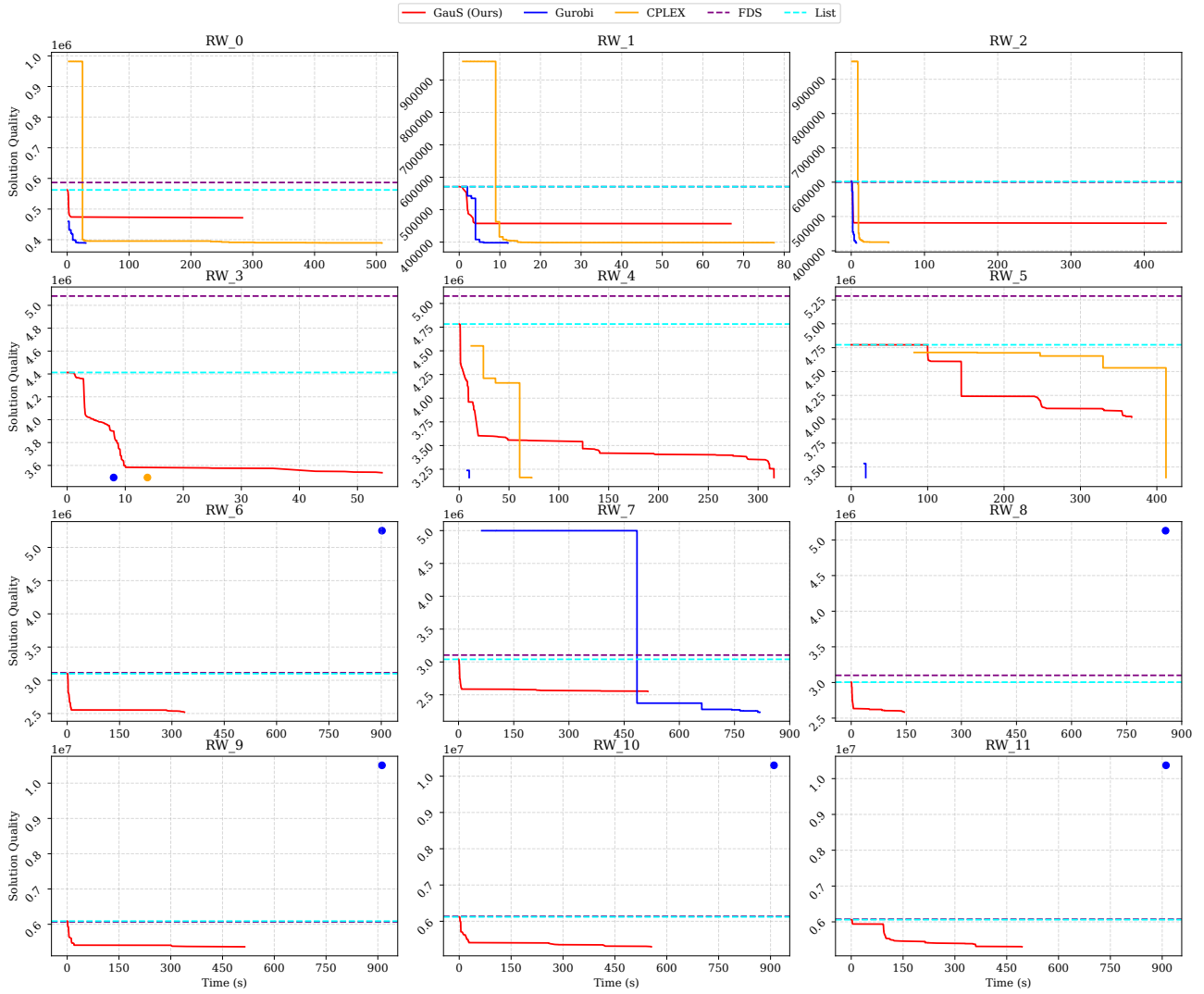


Figure 11. Comprehensive tradeoff comparison of RW on **Formulation B**: Latency constrained, memory footprint optimization — A 15-minute time limit is applied to all methods. Heuristics such as FDS and List Scheduling are represented as horizontal lines to reflect their fast convergence to final solution quality.

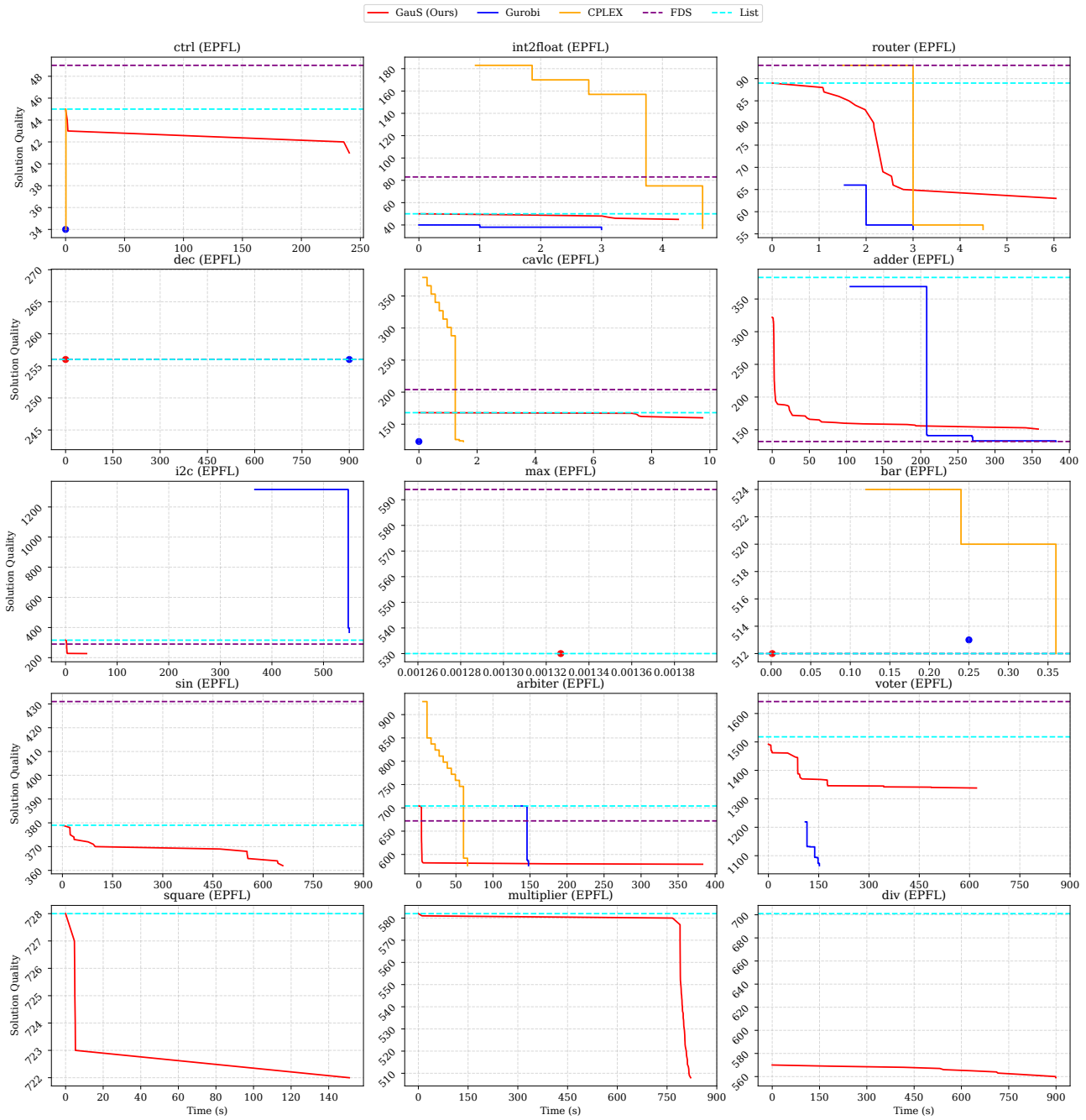


Figure 12. Comprehensive tradeoff comparison of EPFL on **Formulation B**: *Latency constrained, memory footprint optimization* — A 15-minute time limit is applied to all methods. Heuristics such as FDS and List Scheduling are represented as horizontal lines to reflect their fast convergence to final solution quality.

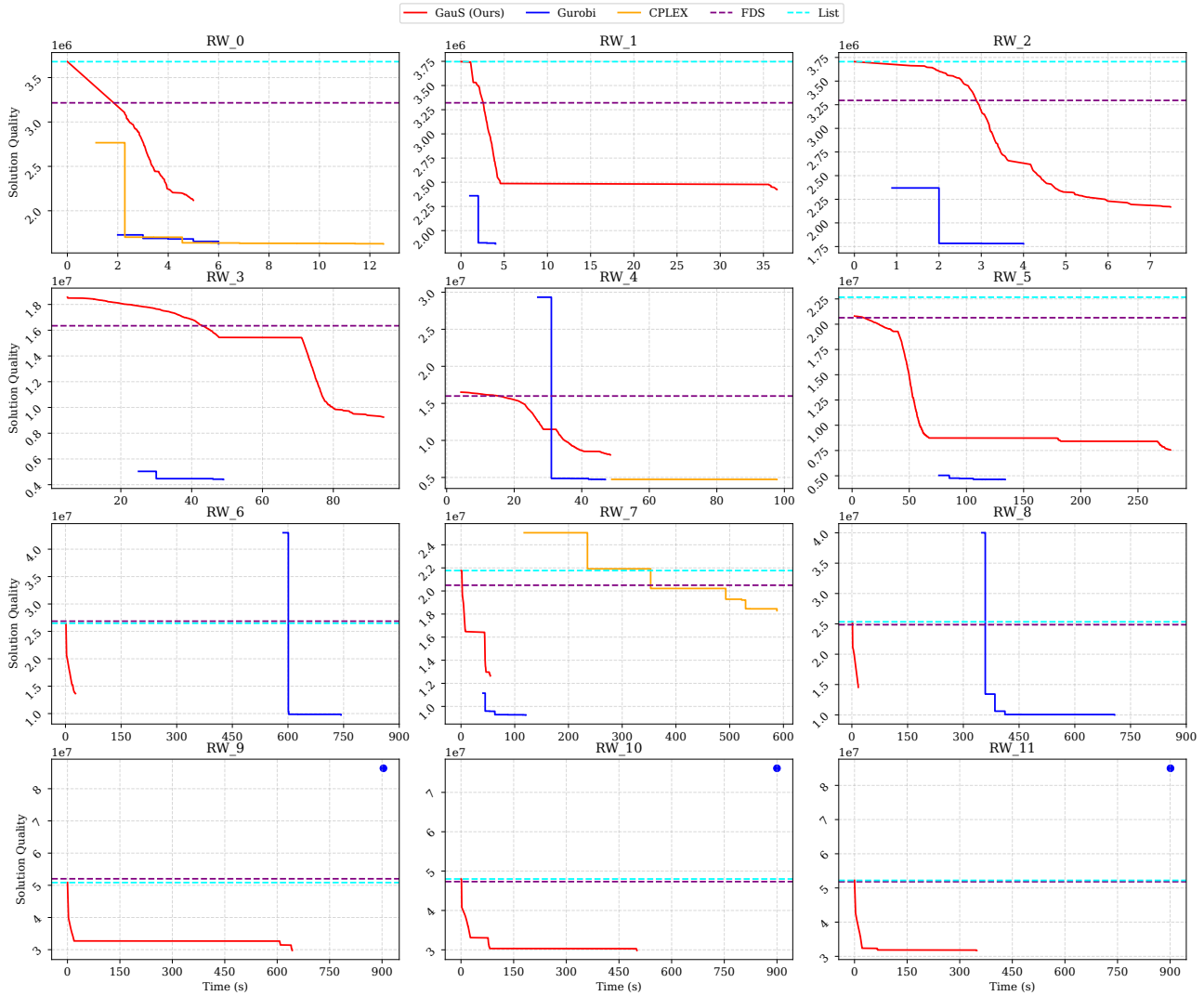


Figure 13. Comprehensive tradeoff comparison of RW on **Formulation C**: Latency, resource, and recurrences constrained, memory footprint modulo optimization — A 15-minute time limit is applied to all methods. Heuristics such as FDS and List Scheduling are represented as horizontal lines to reflect their fast convergence to final solution quality.

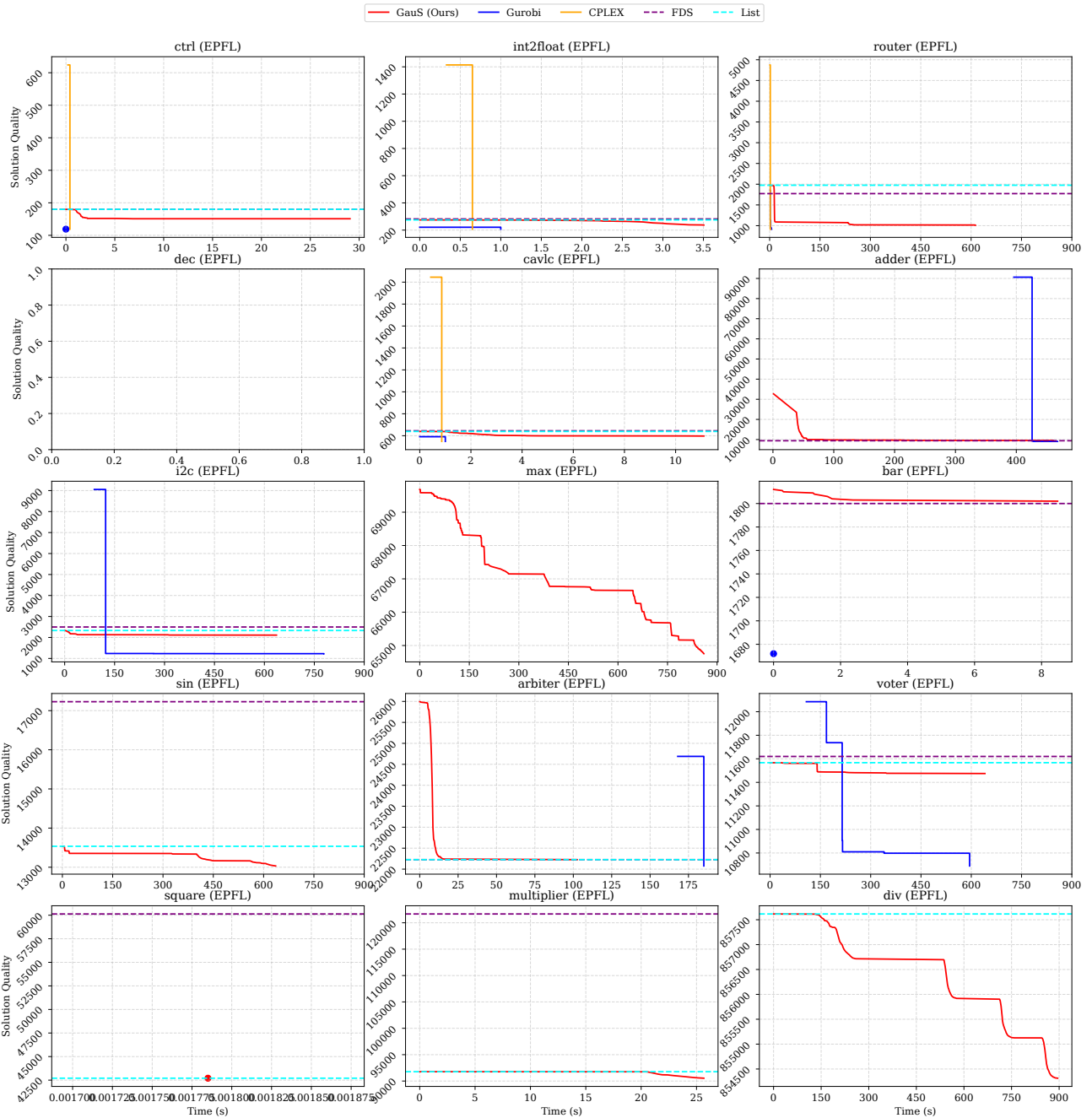


Figure 14. Comprehensive tradeoff comparison of EPFL on **Formulation C**: Latency, resource, and recurrences constrained, memory footprint modulo optimization — A 15-minute time limit is applied to all methods. Heuristics such as FDS and List Scheduling are represented as horizontal lines to reflect their fast convergence to final solution quality. There is no feasible solution for dec, thus plot is left empty.